Quantitative control of a rotary carbon nanotube motor under temperature stimulus

Quantitative control of a rotary carbon nanotube motor under temperature stimulus

Kun Cai[1,2], Jing Wan[1], Qing H Qin[2] and Jiao Shi[1]

[1] College of Water Resources and Architectural Engineering, Northwest A&F University, Yangling 712100, People's Republic of China
[2] Research School of Engineering, The Australian National University, Acton, ACT 2601, Australia

E-mail: qinghua.qin@anu.edu.au

Abstract
Since a double-walled carbon nanotube (DWCNT)-based rotary motor driven by a uniform temperature field was proposed in 2014, how to control quantitatively the rotation of the rotor is still an open question. In this work, we present a mathematical relationship between the rotor's speed and interaction energy. Essentially, the increment of interaction energy between the rotor and the stator(s) determines the rotor's rotational speed, whereas the type of radial deviation of an end carbon atom on the stator determines the rotational direction. The rotational speed of the rotor can be specified by adjusting temperature and radial deviation of an end carbon atom on the stator. It is promising for designing a controllable temperature-driven rotary motor based on DWCNTs with length of few nanometers only.

S Online supplementary data available from stacks.iop.org/NANO/27/055706/mmedia

Keywords: carbon nanotube, rotary nanomotor, molecular dynamics

(Some figures may appear in colour only in the online journal)

1. Introduction

Due to their excellent mechanical properties [1–6] such as ultralow friction and in-shell super-strength, multi-walled carbon nanotubes (MWCNTs) have been widely adopted in constructing nanomotors and nanobearing [1, 7, 8] and strain sensors [9]. Fennimore *et al* [10] were the first to build a true nano-actuator by selecting MWCNTs as a key motion-enabling element. Cai *et al* [11] investigated self-excited oscillation triggered by nonequilibrium attraction of the ends of two tubes. In the electromechanical rotational actuator built by Bourlon *et al* [12], a plate was attached on MWCNTs that acted as a bearing and the actuator was driven to rotate by a charged stator. To avoid an electromigration or random walk effect, Barreiro *et al* [13] built a thermally driven nanomotor based on MWCNTs. In their nanomotor, an outer tube can move by rotation or translation along the axis of inner tubes when a temperature gradient exists along the axis. Motivated by the observation that electron tunneling can cause periodic vibrational [14] and translational motions in molecules [15], Wang *et al* [16] proposed an electron tunneling-driven rotary

nanomotor in which fullerene blades were charged/discharged periodically and driven to rotate in an external electronic field. Optical [17] and chemical methods [18] have also been used to drive the rotary or translational motion of a molecular motor.

Noting that high environmental temperature induces marked thermal vibration of atoms, an easy way to actuate the motion of a molecular motor is to increase temperature. Besides the work by Barreiro *et al* [13], Xu *et al* [19] investigated the motion of a double-walled carbon nanotube (DWCNT)-based motor in a temperature field with thermal fluctuation, observing the rotation of an inner tube within a fixed tube. Guo *et al* [20] studied edge barriers and forces of the interlayer interaction of DWCNTs due to environmental temperature, and found that the edge force is linearly dependent on the temperature. Recently, Cai *et al* [21] studied the thermally driven rotation of the inner tube, including the effects of the differences between the radii of inner and outer tubes, temperature, and the length of the fixed part of the stator. The reported rotational frequency of the rotor was over 160 GHz. That work demonstrated the feasibility of a
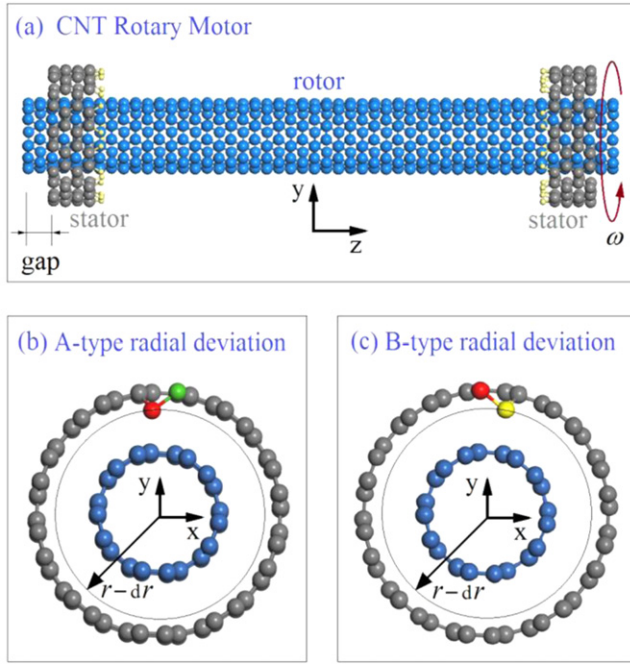
Figure 1. CNT model in simulation. (a) Nanomotor model made from (5, 5)/(10, 10) DWCNTs. The two stators with (10, 10) as outer tubes have C–H bonds on the inside ends, initially. There are 500 and 160 carbon atoms on the rotor and stators, respectively. The yellow atoms are hydrogen atoms, which are bonded with the carbon atoms on the internal edges of the stators. At the start, the system is symmetrical along the central cross-section and the value of the end '*gap*' between the rotor and a stator is 0.25 nm. There are two schemes of radial deviation, i.e., '*dr*', of the radially deviated atom at an outer end of a stator. (b) In 'A-type', the *radially deviated carbon atom* is red. (c) In 'B-type', the radially deviated carbon atom is yellow. The carbon atoms with radial deviation are fixed in position during simulation.

thermally driven motor made from DWCNTs. However, in the models involved in that work, neither the in-depth mechanism of uniform temperature driven rotation nor the quantitative relationship between the rotation of the rotor and the configuration of the system was addressed. In the present study, a quantitative relationship between rotor's speed and interaction energy is presented and used to investigate mechanisms of the DWCNT-based rotary motor driven by temperature stimulus. It provides a feasible way of designing nano-devices whose rotor's rotational speed is controllable.

2. Molecular dynamic simulation

Figure 1(a) shows a model of a nanomotor made from commensurate DWCNTs of (5, 5)/(10, 10). The two parts of the outer tube are arranged near the two ends of the inner tube. At the beginning of each simulation, the tubes are allowed to equilibrate under a Langevin-style thermostat to a specified temperature of 300 K, following energy minimization. After the minimization, the carbon atoms on the stators are fixed and the system is placed in a canonical NVT ensemble for 10 ns of simulation. The time step in the integral of Newton's
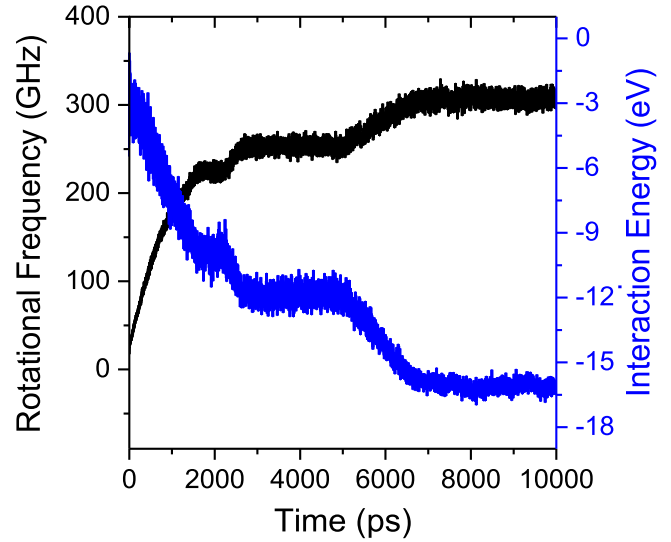
Figure 2. The histories of the rotational frequency of the rotor and the interaction between the rotor and stators.

equation is 1 fs. In this work, molecular dynamics simulation is carried out using LAMMPS [22], AIREBO potential [23] is used to describe the force field.

The radial deviation degree (RDD) represents the asymmetry of the outer tube (stator in figures 1(b) and (c)), which is calculated by the formulation

$$\text{RDD} = \frac{\text{d}r}{l_{c-c}}, \quad (1)$$

where dr is defined in figures 1(b) and (c). $l_{c-c} = 0.142$ nm in this work. When RDD = 0, all the end carbon atoms on the stator are in an ideal circle with the radius of r. A higher value of RDD means that there is a smaller distance between the rotor and stator.

3. Rotational speed of rotor versus interaction energy

The interaction energy is the difference between the potential of the present system and the potentials of the isolated inner tube and two outer tubes. When the atoms in stators are fixed, the interaction energy can also be considered as the increment of the rotor's potential.

From figure 2, the increment of the rotational speed of the rotor is proportional to the increment of the interaction energy of the system, i.e.

$$\Delta\omega = -\alpha \cdot \Delta P_{r-s}, \quad (2)$$

where α is a coefficient depending on temperature and radial deviation of the carbon atom at the outer end of stator.

This phenomenon reveals that the angular acceleration of the rotor is proportional to the interaction power of the system, i.e.

$$\varepsilon = \lim_{\Delta t \to 0} \frac{\Delta\omega}{\Delta t} = -\alpha \cdot \lim_{\Delta t \to 0} \frac{\Delta P_{r-s}}{\Delta t}. \quad (3)$$
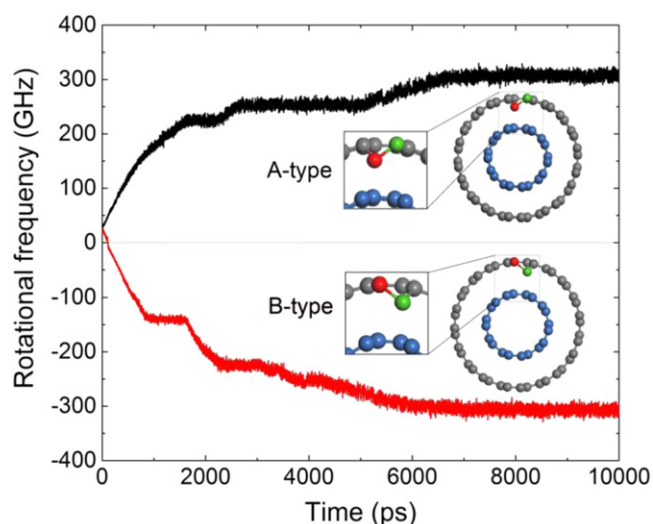
Figure 3. Rotational histories of the rotor in two types of stator, In 'A-type' radial deviation scheme, the red atom on the stator has a RDD of 0.3 (see supplementary movie S1, available at stacks.iop. org/NANO/27/055706/mmedia); in 'B-type' radial deviation scheme, the green atom on the stator has a RDD of 0.3 (see movie S2, available at stacks.iop.org/NANO/27/055706/mmedia). In the system, the red and green atoms are bonded each other.

Equation (3) implies that we can control the acceleration of the rotor's rotation by controlling the variation of interaction energy, i.e., the power, of the system in a design.

4. Rotational direction of rotor

From figure 3, we find that the rotational direction of the rotor in the stators with the 'A-type' scheme is anticlockwise, due to the positive value of rotational frequency. Interestingly, if we adjust the RDD of the green atom on the stator (B-type), the rotational direction is clockwise. It should be mentioned that the hydrogen atoms are bonded with the carbon atoms on the internal ends of stators. After hydrogenation, the edge barrier of potential of the stator is reduced to be close to that of the mid part of the stator. Hence, the rotation of the inner tube is purely due to the interaction of the outer edges of tubes. As a result, we can conclude that the rotational direction (clockwise or anticlockwise) of the rotor is determined by the type of radial deviation, here, including 'A-type' or 'B-type' in figures 1 or 3. This finding implies that we can engender a specified rotational direction of the rotor by selecting the radial deviation type. We also find that the final values of the rotational speed for the two schemes are identical to ~308 GHz when they share the same RDD value.

5. Effect of temperature

In figure 4(a), the histories of the rotational speed of the rotor in the system with the 'A-type' scheme (figure 1(b)) are presented at different environmental temperatures. A higher environmental temperature leads to a higher rotational speed of the rotor. At the same time, the initial value of interaction energy of the system increases with an increase in the environmental temperature (figure 4(b)), and the absolute value of the increment of interaction energy is also more obvious at a higher temperature. Hence, we conclude that a higher temperature leads to a greater decrease in the potential of the system, resulting in a higher speed of rotation of the rotor.
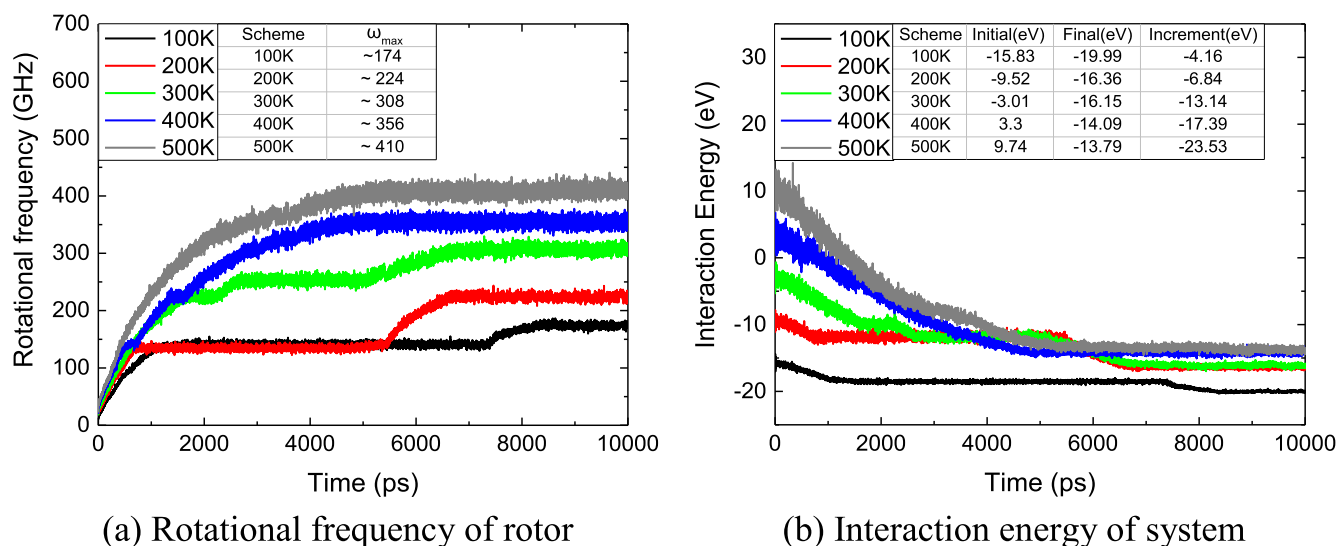
6. Effect of RDD

When the value of RDD varies (figure 5(b)), we find that the absolute value of the increment potential of the system does not always increase with an increase in RDD. Correspondingly, the rotational speed of the rotor has the same characteristics (figure 5(a)). For example, when the RDD is no higher than 0.1, the increment of interaction energy of the system is far less than that when RDD > 0.2. In particular, the absolute value of increment approaches its peak when RDD = 0.4. The rotor's rotational speed is also the highest among the seven schemes. When RDD > 0.4, the absolute value drops. The reason for this phenomenon is that the attraction between rotor and stator increases when the atom on the stator with radial deviation is too close to the rotor. In fact, too high value of RDD leads to sudden stoppage of the rotor [24].
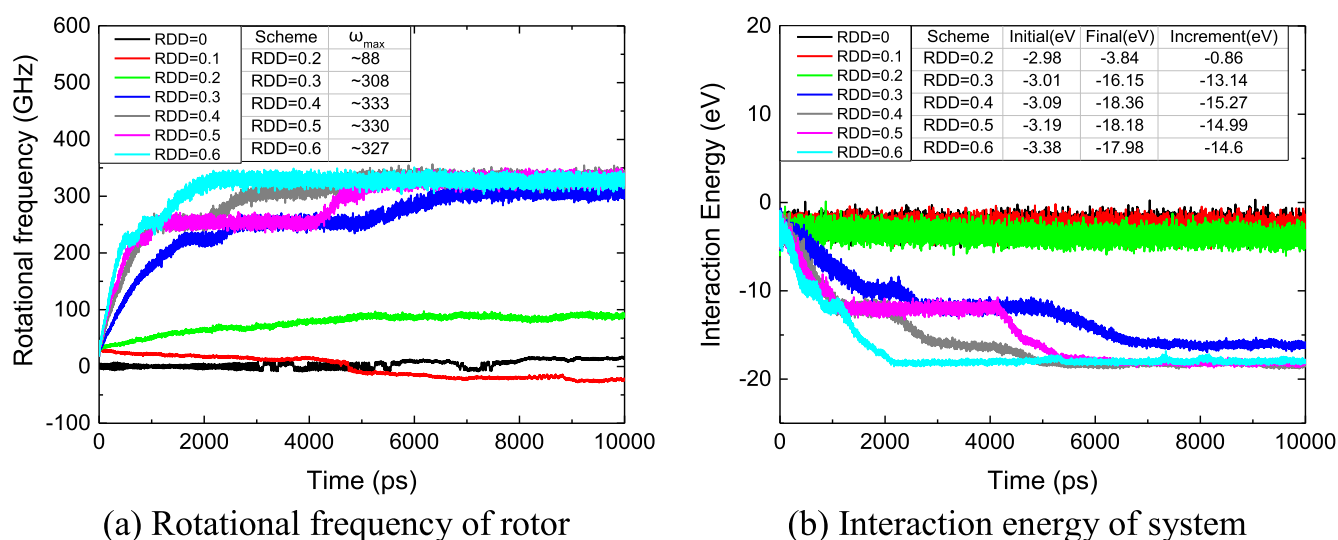
7. Concluding remarks

From the discussion above, we know that the rotational speed of the rotor is determined by the increment of the potential energy of the system. We also know that the interaction energy depends on two factors. One is the charge number of the end carbon atoms, which is fixed in this study. The other is the distance between the rotor and the radially deviated atom on the stator, namely, both the value of gap (figure 1(a), which varies in simulation) and the RDD. Therefore, we can assume that the atoms on the rotor initially vibrate to near its equilibrium state, but the state changes when one of the atoms impacts on the radially deviated atom on the stator. During that impact, a circumferential force appears that causes the rotor to rotate. Higher potential change near the radially deviated atom leads to higher circumferential force. And some conclusions can be drawn.

(1) A higher temperature, or more drastic thermal vibration of atoms on the rotor, leads to a greater change of the potential of system, resulting in a higher speed of rotation of the rotor.
(2) Meanwhile, the type of the radially deviated atom determines the direction of the circumferential force, which is always opposite to the rotational direction (clockwise or anticlockwise) of the rotor.

Scheme	ω_{max}
100K	~174
200K	~ 224
300K	~ 308
400K	~ 356
500K	~ 410

(a) Rotational frequency of rotor

Scheme	Initial(eV)	Final(eV)	Increment(eV)
100K	-15.83	-19.99	-4.16
200K	-9.52	-16.36	-6.84
300K	-3.01	-16.15	-13.14
400K	3.3	-14.09	-17.39
500K	9.74	-13.79	-23.53

(b) Interaction energy of system

Figure 4. At different temperatures, histories of the rotational speed of the rotor and the interaction energy in the system and RDD = 0.3.

Scheme	ω_{max}
RDD=0.2	~88
RDD=0.3	~308
RDD=0.4	~333
RDD=0.5	~330
RDD=0.6	~327

(a) Rotational frequency of rotor

Scheme	Initial(eV)	Final(eV)	Increment(eV)
RDD=0.2	-2.98	-3.84	-0.86
RDD=0.3	-3.01	-16.15	-13.14
RDD=0.4	-3.09	-18.36	-15.27
RDD=0.5	-3.19	-18.18	-14.99
RDD=0.6	-3.38	-17.98	-14.6

(b) Interaction energy of system

Figure 5. Histories of rotational speed of the rotor and the interaction energy in the system at different values of RDD.

(3) The absolute value of the potential increment of the system does not always increases with an increase in the RDD. For example, the absolute value approaches its peak when the RDD equals 0.4.

By adjusting either environmental temperature or RDD, the rotor with a specified rotational speed can be obtained. The rotational direction can also be adjusted by varying the RDD type.

8. Acknowledgments

References

[1] Cumings J and Zettl A 2000 Low-friction nanoscale linear bearing realized from multiwall carbon nanotubes *Science* **289** 602–4
[2] Zhang R, Ning Z, Zhang Y, Zheng Q, Chen Q, Xie H, Zhang Q, Qian W and Wei F 2013 Superlubricity in centimetres-long double-walled carbon nanotubes under ambient conditions *Nat. Nanotechnology* **8** 912–6
[3] Qiu W, Kang Y L, Lei Z K, Qin Q H and Li Q 2009 A new theoretical model of a carbon nanotube strain sensor *Chin. Phys. Lett.* **26** 080701
[4] Popov A M, Lebedeva I V, Knizhnik A A, Lozovik Y E and Potapkin B V 2013 *Ab initio* study of edge effect on relative motion of walls in carbon nanotubes *J. Chem. Phys.* **138** 024703
[5] Qian D, Wagner G J, Liu W K, Yu M F and Ruoff R S 2002 Mechanics of carbon nanotubes *Appl. Mech. Rev.* **55** 495–533

[6] Qin Z, Qin Q H and Feng X Q 2008 Mechanical property of carbon nanotubes with intramolecular junctions: molecular dynamics simulations *Phys. Lett.* A **372** 6661–6

[7] Cai K, Zhang X, Shi J and Qin Q H 2015 Temperature effects on a motion transmission device made from carbon nanotubes: a molecular dynamics study *RSC Adv.* **5** 66438–50

[8] Yin H, Cai K, Wei N, Qin Q H and Shi J 2015 Study on the dynamics responses of a transmission system made from carbon nanotubes *J. Appl. Phys.* **117** 234305

[9] Qiu W, Li Q, Lei Z, Qin Q H, Deng W and Kang Y 2013 The use of a carbon nanotube sensor for measuring strain by micro-Raman spectroscopy *Carbon* **53** 161–8

[10] Fennimore A M, Yuzvinsky T D, Han W Q, Fuhrer M S, Cumings J and Zettl A 2003 Rotational actuators based on carbon nanotubes *Nature* **424** 408–10

[11] Cai K, Yin H, Qin Q H and Li Y 2014 Self-excited oscillation of rotating double-walled carbon nanotubes *Nano Lett.* **14** 2558–62

[12] Bourlon B, Glattli D C, Miko C, Forro L and Bachtold A 2004 Carbon nanotube based bearing for rotational motions *Nano Lett.* **4** 709–12

[13] Barreiro A, Rurali R, Hernandez E R, Moser J, Pichler T, Forro L and Bachtold A 2008 Subnanometer motion of cargoes driven by thermal gradients along carbon nanotubes *Science* **320** 775–8

[14] Park H, Park J, Lim A K L, Anderson E H, Alivisatos A P and McEuen P L 2000 Nanomechanical oscillations in a single-C-60 transistor *Nature* **407** 57–60

[15] Kaun C C and Seideman T 2005 Current-driven oscillations and time-dependent transport in nanojunctions *Phys. Rev. Lett.* **94** 226801

[16] Wang B, Vukovic L and Kral P 2008 Nanoscale rotary motors driven by electron tunneling *Phys. Rev. Lett.* **101** 186808

[17] Tan S D, Lopez H A, Cai C W and Zhang Y G 2004 Optical trapping of single-walled carbon nanotubes *Nano Lett.* **4** 1415–9

[18] Kelly T R, De Silva H and Silva R A 1999 Unidirectional rotary motion in a molecular system *Nature* **401** 150–2

[19] Xu Z, Zheng Q S and Chen G 2007 Thermally driven large-amplitude fluctuations in carbon-nanotube-based devices: molecular dynamics simulations *Phys. Rev. B* **75** 195445

[20] Guo Z, Chang T, Guo X and Gao H 2011 Thermal-induced edge barriers and forces in interlayer interaction of concentric carbon nanotubes *Phys. Rev. Lett.* **107** 105502

[21] Cai K, Li Y, Qin Q H and Yin H 2014 Gradientless temperature-driven rotating motor from a double-walled carbon nanotube *Nanotechnology* **25** 505701

[22] LAMMPS 2013 Molecular Dynamics Simulator (http://lammps.sandia.gov/)

[23] Stuart S J, Tutein A B and Harrison J A 2000 A reactive potential for hydrocarbons with intermolecular interactions *J. Chem. Phys.* **112** 6472–86

[24] Cai K, Yu J, Yin H and Qin Q H 2015 Sudden stoppage of rotor in a thermally driven rotary motor made from double-walled carbon nanotubes *Nanotechnology* **26** 095702